Endocannabinoids Modulate Human Epidermal Keratinocyte Proliferation and Survival via the Sequential Engagement of Cannabinoid Receptor-1 and Transient Receptor Potential Vanilloid-1

Balázs I. Tóth[1], Nóra Dobrosi[1], Angéla Dajnoki[1], Gabriella Czifra[1], Attila Oláh[1], Attila G. Szöllősi[1], István Juhász[2], Koji Sugawara[3], Ralf Paus[3,4] and Tamás Bíró[1]

We have recently shown that lipid mediators of the emerging endocannabinoid system (ECS) are key players of growth control of the human pilosebaceous unit. In this study, we asked whether the prototypic endocannabinoid anandamide (*N*-arachidonoylethanolamine, AEA) has a role in growth and survival of epidermal keratinocytes (KCs). Using human cultured KCs and skin organ-culture models, and by employing combined pharmacological and molecular approaches, we provide early evidence that AEA markedly suppresses KC proliferation and induces cell death, both *in vitro* and *in situ*. Moreover, we present that these cellular actions are mediated by a most probably constitutively active signaling mechanism that involves the activation of the metabotropic cannabinoid receptor CB_1 and a sequential engagement of the "ionotropic cannabinoid receptor" transient receptor potential vanilloid-1 (TRPV1). Finally, we demonstrate that the cellular effects of AEA are most probably due to a Ca^{2+} influx via the non-selective, highly Ca^{2+}-permeable ion channel TRPV1, and the concomitant elevation of intracellular Ca^{2+} concentration. The data reported here may encourage one to explore whether the targeted manipulation of the above signaling pathway of the cutaneous ECS could become a useful adjunct treatment strategy for hyperproliferative human dermatoses such as psoriasis or KC-derived skin tumors.

Journal of Investigative Dermatology (2011) **131,** 1095–1104; doi:10.1038/jid.2010.421; published online 20 January 2011

INTRODUCTION

The emerging endocannabinoid system (ECS, Mechoulam *et al.*, 1998; Howlett *et al.*, 2002; Pacher *et al.*, 2006; Di Marzo, 2008) has lately been identified in the skin. Indeed, several human skin cell compartments produce prototypic endocannabinoids such as anandamide (*N*-arachidonoylethanolamine, AEA) and 2-arachidonoylglycerol, and express enzymes involved in the synthesis and metabolism of these lipid mediators (Calignano *et al.*, 1998; Berdyshev *et al.*, 2000; Maccarrone *et al.*, 2003; Karsak *et al.*, 2007). Furthermore, the G-protein-coupled metabotropic cannabinoid receptors (CB_1 and CB_2; Pertwee, 2005; Howlett, 2005; Mackie, 2006) as well as, to our knowledge, previously unreported, ''ionotropic cannabinoid receptors'' (such as transient receptor potential vanilloid-1, TRPV1; Di Marzo *et al.*, 1998, 2001; Zygmunt *et al.*, 1999) were identified, both *in situ* and *in vitro*, on numerous skin cell populations such as epidermal and hair follicle keratinocytes (KCs) and sebaceous gland-derived sebocytes (Casanova *et al.*, 2003; Bodó *et al.*, 2005; Ibrahim *et al.*, 2005; Stander *et al.*, 2005; Blazquez *et al.*, 2006; Karsak *et al.*, 2007; Telek *et al.*, 2007; Dobrosi *et al.*, 2008; Tóth *et al.*, 2009). These discoveries have made the ECS a topic of major interest in cutaneous neuroendocrinology and neuropharmacology (Bíró *et al.*, 2009; Kupczyk *et al.*, 2009).

The ECS is profoundly involved in the regulation of human epidermal homeostasis. Indeed, AEA inhibited the differentiation of cultured normal human epidermal KCs (NHEKs) and HaCaT KCs whose effect was mediated by increasing DNA methylation through mitogen-activated protein kinase-dependent pathways (p38, p42/44) triggered

[1]*Department of Physiology, Medical and Health Science Center, Research Center for Molecular Medicine, University of Debrecen, Debrecen, Hungary;* [2]*Department of Dermatology, Medical and Health Science Center, Research Center for Molecular Medicine, University of Debrecen, Debrecen, Hungary;* [3]*Department of Dermatology, University of Lübeck, Lübeck, Germany and* [4]*Epithelial Sciences, School of Translational Medicine, University of Manchester, Manchester, UK*

Correspondence: Tamás Bíró, Department of Physiology, Medical and Health Science Center, Research Center for Molecular Medicine, University of Debrecen, Nagyerdei Körút 98, PO Box 22, Debrecen 4032, Hungary. E-mail: biro@phys.dote.hu

Abbreviations: AEA, N-arachidonoylethanolamine; $[Ca^{2+}]_i$, intracellular Ca^{2+} concentration; CAPS, capsaicin; ECS, endocannabinoid system; FLIPR, fluorescence image plate reader; G6PD, glucose-6-phosphate dehydrogenase; KC, keratinocyte; NHEK, normal human epidermal KC; RNAi, RNA interference; TRPV1, transient receptor potential vanilloid-1; TTP, time to peak

Received 12 July 2010; revised 29 October 2010; accepted 16 November 2010; published online 20 January 2011

by CB_1 activation (Maccarrone *et al.*, 2003; Paradisi *et al.*, 2008). Involvement of CB_1 in the regulation of epidermal differentiation is also suggested by the differential *in situ* expression of CB_1 in the human epidermis, with it being higher in the more differentiated (granular and spinous) layers (Casanova *et al.*, 2003; Stander *et al.*, 2005).

Published data on CB-coupled mechanisms in the regulation of epidermal KC proliferation appear to be conflicting. For example, phytocannabinoids (for example, Δ^9-tetrahydrocannabinol) derived from the plant *Cannabis sativa* as well as synthetic CB agonists inhibited growth of cultured transformed (HPV-16 E6/E7) human epidermal KCs; yet, these effects were $CB_{1/2}$ independent (Wilkinson and Williamson, 2007). In contrast, on tumorigenic transformed murine KCs (PDV.C57 and HaCa4), the growth-inhibitory actions of synthetic CB agonists were prevented by both CB_1 and CB_2 antagonists (Casanova *et al.*, 2003). Interestingly, synthetic CB_1 and CB_2 agonists were reportedly ineffective in modulating cellular growth of both cultured NHEKs and non-tumorigenic human (HaCaT) and murine (MCA3D) KCs (Casanova *et al.*, 2003).

However, none of the above studies have investigated the role of endocannabinoids in the regulation of human epidermal KC proliferation. Therefore, in this study, we have investigated the actions of the most extensively studied endocannabinoid, AEA, on the biology of human KCs. Our specific aims were to (i) define the *in vitro* and *in situ* effects of AEA on epidermal KC growth and survival; and (ii) identify those intracellular signaling pathways that may mediate the actions of the endocannabinoid. To achieve these goals, we used human cultured KCs (NHEKs, HaCaTs) and skin organ-culture models and employed combined pharmacological and molecular approaches.

RESULTS

Cultured human KCs express CB_1, CB_2, and TRPV1

First, we sought to identify the existence of putative AEA target molecules on human KCs that were shown to express ECS (Maccarrone *et al.*, 2003; Petrosino *et al.*, 2010). Expressions of CB_1 and CB_2 were unambiguously identified, both on NHEK and HaCaT KCs, using complementary immunocytochemistry and western blotting techniques (Figure 1a and b). Likewise, the ''ionotropic AEA-receptor'' TRPV1 was also detected on these cells (Figure 1a and b). This corresponded well to expression of the *CB_1* and *CB_2* genes in both types of KCs, as demonstrated by RT-PCR (Figure 1c) and by quantitative ''real-time'' PCR (Supplementary Figure 1 online; see also Supplementary Data online for the Materials and Methods).

AEA inhibits human KC growth and induces cell death

We then investigated the effects of the endocannabinoid on growth and survival of KCs. We found that AEA dose-dependently reduced ($P<0.05$, $n=4$ in each experiment) cell viability and proliferation of both NHEK and HaCaT cells (Figure 2a). To assess whether this effect was due to the induction of cell death (apoptosis and/or necrosis), a series of functional assays was performed. As measured by quantitative fluorimetric determinations (as well as by complementary immunofluorescence (data not shown)), AEA markedly ($P<0.05$) and dose-dependently increased the number of Annexin-V-positive cells (Figure 2b). Moreover, the endocannabinoid AEA markedly decreased mitochondrial membrane potential (Figure 2c) and induced the activation of pro-apoptotic caspases (Figure 2d), another hallmark of apoptosis. Of further importance, highest concentrations of AEA were also able to significantly ($P<0.05$) increase Sytox Green accumulation (Figure 2e) and glucose-6-phosphate dehydrogenase (G6PD) release (Figure 2f), two complementary indicators of necrosis/cytotoxicity. These findings suggested that AEA induced cell death of human KCs *in vitro*.

AEA inhibits proliferation and induces apoptosis of epidermal KCs *in situ*

Next, we employed the organ culture of normal, full-thickness human skin fragments (Lu *et al.*, 2007; Tiede *et al.*, 2009). After treatment with AEA, double Ki67/TUNEL immunolabeling was performed to simultaneously assess the *in situ* effects of AEA on human KC proliferation and apoptosis. As shown in Figure 3, perfectly in line with the above-mentioned cell culture results, AEA treatment markedly ($P<0.05$) suppressed the percentage of proliferating (Ki67+) cells, whereas it dramatically increased that of apoptotic (TUNEL+) cells in normal human epidermis organ cultured under serum-free conditions.

Cellular actions of AEA are mediated by CB_1 and TRPV1

We then investigated the involvement of ''AEA-receptors'' in mediating the cellular actions of the endocannabinoid. As AEA can stimulate both CBs and TRPV1, first, cultured human KCs were treated with highly selective inhibitors of defined CB subtypes (AM251 for CB_1 and AM630 for CB_2) or TRPV1 (capsazepine, iodoresiniferatoxin). Figure 4a shows that these inhibitors did not reduce viability of the cells. However, inhibition of CB_1 and TRPV1, but notably not of CB_2 alone, markedly abrogated the growth-inhibitory and apoptosis-inducing cellular effects of AEA ($P<0.05$; Figure 4b–d). Likewise, suppression of extracellular [Ca^{2+}] also prevented the cellular actions of AEA (Figure 4b–d), further supporting the involvement of the Ca^{2+}-permeable ion channel TRPV1. (Suppression of extracellular [Ca^{2+}] did not change the viability of the cells (data not shown).)

To further assess the roles of CB_1 and TRPV1, a series of receptor knockdown experiments was carried out in accordance with the techniques developed in our previous studies, which were optimized for various cultured skin cells (Dobrosi *et al.*, 2008; Tóth *et al.*, 2009). (The efficacy of the specific RNA interference (RNAi)-mediated silencing is shown in Supplementary Figure 2 online.) Scrambled RNAi probes or RNAi oligonucleotides against CB_1, CB_2, and TRPV1 did not decrease human KC viability in culture (Figure 5a). In contrast, RNAi-mediated silencing of CB_1 and TRPV1 moderately, yet significantly ($P<0.05$), stimulated KC growth (Figure 5a). This latter finding suggested that CB_1 and TRPV1 may function as constitutively active and/or continuously activated receptors (by endogenous ligands produced, for

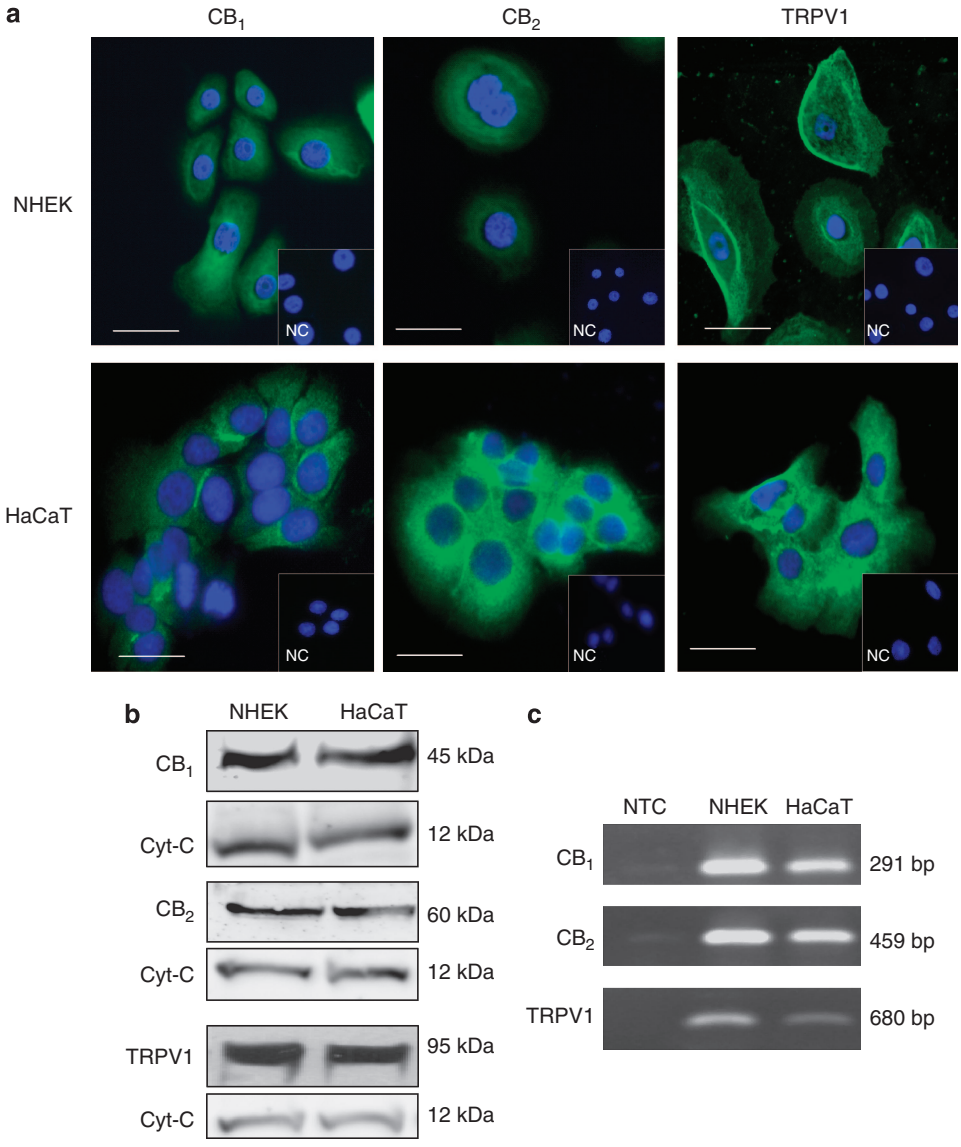

Figure 1. CB_1, CB_2, and transient receptor potential vanilloid-1 (TRPV1) are expressed on cultured human keratinocytes (KCs). (**a**) Specific immunoreactivity of CB_1, CB_2, and TRPV1 on normal human epidermal (NHEK; upper row) and HaCaT KCs (lower row), as determined by immunofluorescence (FITC, green fluorescence). Nuclei were counterstained with DAPI (4′,6-diamidino-2-phenylindole; blue fluorescence). NC, pre-absorption negative control. Bar = 10 μm. (**b**) Western blot analysis. Expressions of CB_1, CB_2, and TRPV1 were determined on cell lysates of NHEK and HaCaT KCs. Cytochrome *c* (Cyt-C) served as loading control. (**c**) RT-PCR analysis of CB_1, CB_2, and TRPV1 mRNA transcripts. NTC, non-template control. In all cases, three to five additional experiments yielded similar results.

example, by KCs; Maccarrone *et al.*, 2003; Petrosino *et al.*, 2010) to inhibit the growth of epidermal KCs.

Similar to the above pharmacological data, silencing of CB_1 or TRPV1 (but, not of CB_2) counteracted AEA's negative effect on cell viability (Figure 5b) and the induction of apoptosis (Figure 5c and d). These data further argued in support of a simultaneous involvement of both CB_1- and TRPV1-mediated signaling.

A sequential signaling pathway ($CB_1 \rightarrow TRPV1 \rightarrow Ca^{2+}$ influx) mediates the actions of AEA on human KCs

Intriguingly, the co-administration of CB_1 and TRPV1 antagonists (Figure 4b–d) or the simultaneous RNAi-mediated silencing of CB_1 and TRPV1 (Figure 5b–d) did not exert additive effects in preventing the cellular actions of AEA. This suggested that AEA does not co-activate CB_1 and TRPV1, but rather induces sequential activation of either receptor (that is, $CB_1 \rightarrow TRPV1$, or $TRPV1 \rightarrow CB_1$), which then mediates the complex actions of the endocannabinoid.

As TRPV1 functions as a Ca^{2+}-permeable ion channel on KCs as well (Southall *et al.*, 2003; Bodó *et al.*, 2005), Ca^{2+}-imaging experiments were performed to test whether AEA is capable of elevating the intracellular Ca^{2+} concentration ($[Ca^{2+}]_i$). As a positive control, we employed the TRPV1 agonist capsaicin (CAPS), which increases $[Ca^{2+}]_i$ in KCs (Southall *et al.*, 2003; Bodó *et al.*, 2005).

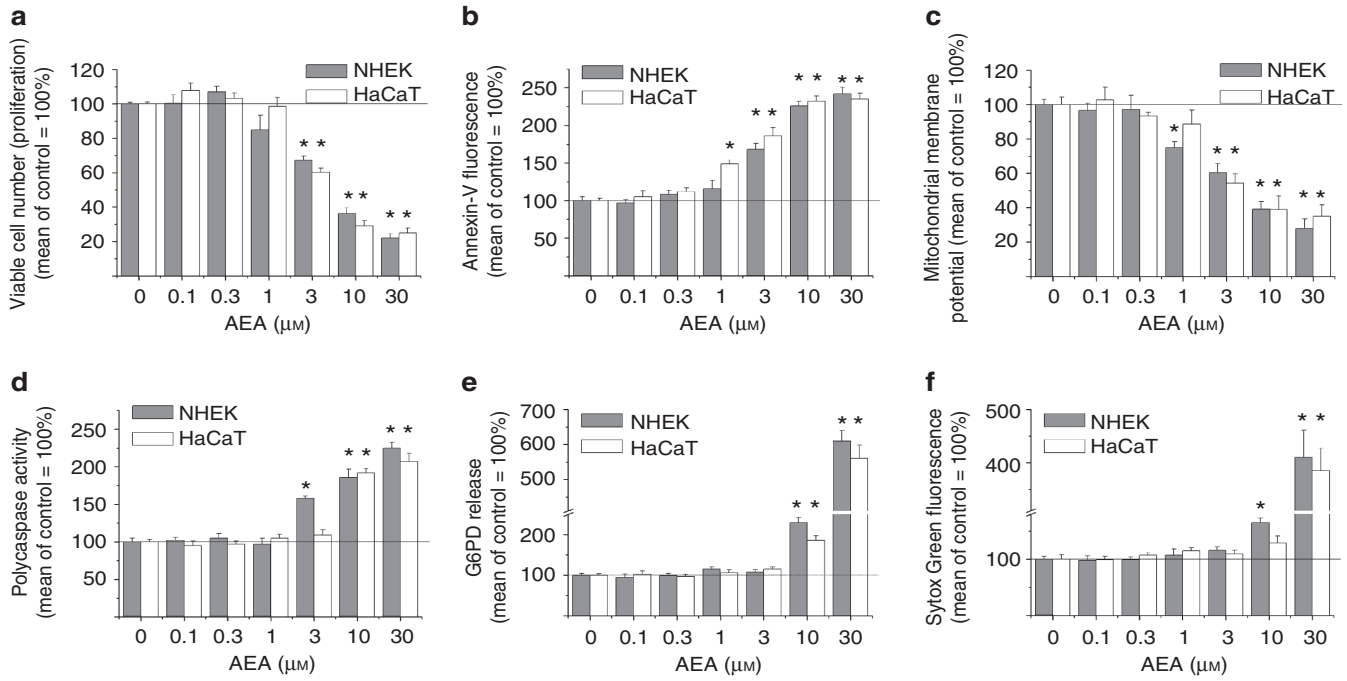

Figure 2. *N*-arachidonoylethanolamine (AEA) suppresses cellular viability and proliferation, and induces cell death of cultured human keratinocytes (KCs). KCs were treated with various concentrations of AEA for 24 hours. (**a**) Determination of viable cell number by colorimetric MTT (3-(4,5-dimethylthiazol-2-yl)-2,5-diphenyltetrazolium bromide) assay. Quantitative measurement of apoptosis by (**b**) Annexin-V assay reflecting phosphatidylserine translocation; (**c**) $DiIC_1(5)$ assay reflecting mitochondrial membrane potential; (**d**) polycaspase assay reflecting activation of pro-apoptotic caspases. Quantitative measurement of necrosis by (**e**) glucose-6-phosphate dehydrogenase (G6PD) release assay and (**f**) Sytox Green assay. In all cases, data (mean ± SEM) are expressed as a percentage of the mean value (defined as 100%) of the vehicle-treated control group. For statistical analysis, * marks significant ($P<0.05$) differences compared with the vehicle-treated control group; $n=4$ in each group. Three to four additional experiments yielded similar results. NHEK, normal human epidermal KC.

AEA indeed induced transient elevations of $[Ca^{2+}]_i$ in a dose-dependent manner (Figure 6a). Of note, the amplitude of the maximal AEA-induced $[Ca^{2+}]_i$ elevation was in the range of that evoked by 10 μM CAPS (Figure 6a). However, the kinetics of the AEA- and the CAPS-induced cellular actions were markedly different. Namely, the effect of AEA was realized only after a long-term incubation of the cells (time-to-peak, TTP, value of 168.2 ± 20 seconds, mean ± SEM, $n=16$ cells), in contrast to the fast action of the TRPV1 agonist CAPS (TTP of 13.8 ± 4 seconds, mean ± SEM, $n=11$ cells; Figure 6b).

Of further importance, the AEA-evoked $[Ca^{2+}]_i$ transients were completely prevented by administering the TRPV1 antagonists capsazepine or iodoresiniferatoxin, or by suppression of extracellular $[Ca^{2+}]$ (Figure 6c). These findings further suggested that AEA induced a TRPV1-mediated Ca^{2+} influx. Likewise, the effect of AEA to raise $[Ca^{2+}]_i$ was also fully abrogated by the CB_1 antagonist AM-251 (Figure 6c). This argued for the fact that, besides TRPV1, CB_1-coupled signaling is also involved in mediating the effect of AEA to elevate $[Ca^{2+}]_i$. Finally, we have also found that co-administration of CB_1 and TRPV1 antagonists did not exert an additive inhibitory effect (Figure 6c).

Intriguingly, CB_1 and TRPV1 inhibitors behaved in a different way on the TTP value of the transients. Namely, the TRPV1 ''channel antagonists'' capsazepine and iodoresiniferatoxin did not affect the TTP value of AEA-induced $[Ca^{2+}]_i$ responses (Figure 6b). In striking contrast, the selective CB_1 antagonist AM-251 further markedly increased (the already long) TTP value by almost threefold (Figure 6b). (Instead, the CB_2 antagonist AM-630 had no effect on either the amplitude or the TTP of the AEA-evoked $[Ca^{2+}]_i$ elevations; Figure 6b and c.) Finally, as expected, we also found that the effect of CAPS to raise $[Ca^{2+}]_i$ was markedly abrogated by the TRPV1 inhibitors as well as by suppression of extracellular $[Ca^{2+}]$, whereas it was not affected by antagonists of CB_1 or CB_2 (Figure 6d).

DISCUSSION

Uncovering the as yet ill-characterized functions of the ECS in human skin biology and pathology is an important, integral part of the ongoing exploration of the skin as a non-classical neuroendocrine organ (Slominski and Wortsman, 2000; Slominski *et al.*, 2008). In this context, we provide evidence that the prototypic endocannabinoid AEA—which, as detailed above, is synthesized in several human skin cell compartments—inhibits proliferation and induces cell death of human epidermal KCs in cultures as well as *in situ*. We also show that AEA-induced KC death is Ca^{2+} dependent. These data support the concept that KCs exploit a physiologically relevant ECS for negatively regulating their own growth in a paracrine and/or autocrine manner.

Furthermore, we show that the KC death-promoting effects of AEA are mediated by a sequentially engaged signaling

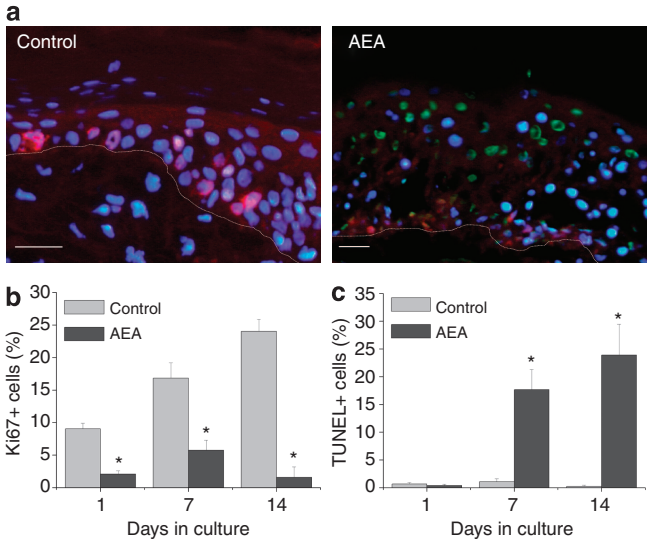

Figure 3. *N*-arachidonoylethanolamine (AEA) suppresses proliferation and induces apoptosis of human keratinocytes (KCs) *in situ*. Human skin organ cultures were treated for 1, 7, and 14 days by vehicle (Control) or 30 μM AEA. Cryostat sections were prepared and co-immunolabeling of proliferating (Ki67 +) and apoptotic (TUNEL +) cells was performed. (**a**) Representative immunofluorescence images of the epidermis after 14 days treatment. Ki67 + cells: red fluorescence, TUNEL + cells: green fluorescence. Nuclei were counterstained with DAPI (4′,6-diamidino-2-phenylindole; blue fluorescence). Dotted lines represent the border of epidermis and dermis. Bars = 25 μm. (**b**,**c**) Statistical analysis of number of Ki-67 + (**b**) and TUNEL + (**c**) cells, as compared with the number of DAPI + epidermal cells on 10 sections per group. Data are expressed as mean ± SEM. * Marks significant ($P<0.05$) differences compared with the vehicle-treated control group. Three additional experiments yielded similar results.

mechanism ($CB_1 \rightarrow TRPV1 \rightarrow Ca^{2+}$ influx). This model is supported by several lines of evidence:

(i) Both CB_1 and TRPV1 antagonists, the suppression of extracellular $[Ca^{2+}]$, and RNAi-mediated silencing of these receptors were able to prevent the cellular actions of AEA.

(ii) However, these pharmacological and molecular inhibitory effects were not additive, arguing for the lack of co-activation of CB_1 and TRPV1 by AEA.

(iii) The effect of AEA to increase $[Ca^{2+}]_i$ was realized only after a long-term incubation of the cells, in contrast to the immediate action of the ''direct'' TRPV1 agonist CAPS. Although we cannot exclude the possibility that anandamide exhibited a slower onset of action due to its higher lipophilicity, as compared with that of CAPS (as nicely shown by Lazar *et al.*, 2006 and Ursu *et al.*, 2010), these results suggest that AEA may not directly activate TRPV1, but rather multiple (and yet to be determined) AEA-evoked signaling pathways are involved in the opening of the ion channel.

(iv) That these ''upstream'' mechanisms involve the preceding action of AEA on CB_1 is supported by the fact that, whereas both CB1 and TRPV1 antagonists were able to equally suppress the amplitude of the AEA-induced $[Ca^{2+}]_i$ elevations, the CB_1 antagonist AM-251 (unlike the ''channel antagonists'' of TRPV1 that do not affect the activity of CB_1) markedly increased the already very long TTP value of the $[Ca^{2+}]_i$ transients.

(v) Finally, we found that the effect of CAPS to raise $[Ca^{2+}]_i$ was inhibited by TRPV1 antagonists and by suppression of extracellular $[Ca^{2+}]$, but not by antagonists of CB_1, which argues for the lack of an ''other way around'' sequential mechanism of $AEA \rightarrow TRPV1 \rightarrow CB_1 \rightarrow Ca^{2+}$ influx.

This sequential activation mechanism, at least in part, is similar to those described in other cellular systems. Using cells ectopically co-expressing CB_1 and TRPV1, Hermann *et al.* (2003) have elegantly shown that CB_1 agonists, depending on the activity of the cAMP-coupled signaling mechanisms, may significantly modulate the Ca^{2+} influx mediated by TRPV1. Likewise, in experiments employing *CB_1* gene-deficient mice, it was shown that constitutive activity at the CB_1 receptor was required to maintain the TRPV1 receptor in a ''sensitized'' state (Fioravanti *et al.*, 2008).

As inhibition or RNAi-mediated silencing of CB_2 did not affect the cellular actions of AEA (which, otherwise, may also activate CB_2; Pertwee, 2005; Mackie, 2006), it appears that CB_2 is not involved in mediating the growth-inhibitory effect of AEA on human epidermal KCs. These results were in line with previous findings showing that CB_1, but not CB_2, has a pivotal role in regulation of epidermal differentiation of human KCs (Paradisi *et al.*, 2008). However, CB_2-mediated signaling on KCs was shown to be involved in anti-nociception (by the release of endogenous opioids which, in turn, inhibit pain-sensing skin afferent fibers; Ibrahim *et al.*, 2005) and in various forms of cutaneous inflammation (Oka *et al.* 2006; Karsak *et al.*, 2007).

The fact that RNAi-mediated silencing of CB_1 and TRPV1 significantly promoted the growth of human KCs suggests that the joint CB_1-TRPV1 signaling pathway identified here functions as a previously unknown, endogenously active receptor-channel mechanism that constitutively keeps human KC proliferation in check. Therefore, the fine-tuned endogenous ECS tone of the skin—set by constant or on-demand production of locally synthesized endocannabinoids—not only controls, for example, cutaneous immune competence and/or tolerance, lipid homeostasis, or adnexal biology (reviewed in Bíró *et al.*, 2009; Kupczyk *et al.*, 2009) but also regulates epidermal homeostasis. Obviously, subsequent studies will need to support the physiological relevance of this, to our knowledge, previously unreported concept by direct *in vivo* evidence. Likewise, it deserves systematic analysis of whether dysfunctions in the cutaneous ECS can trigger or aggravate chronic hyperproliferative, pruritic, and/or pro-inflammatory skin diseases. Along these lines, the data reported here certainly encourage one to explore whether the targeted manipulation of the ECS could become a useful adjunct treatment strategy for hyperproliferative human dermatoses such as psoriasis or KC-derived skin tumors.

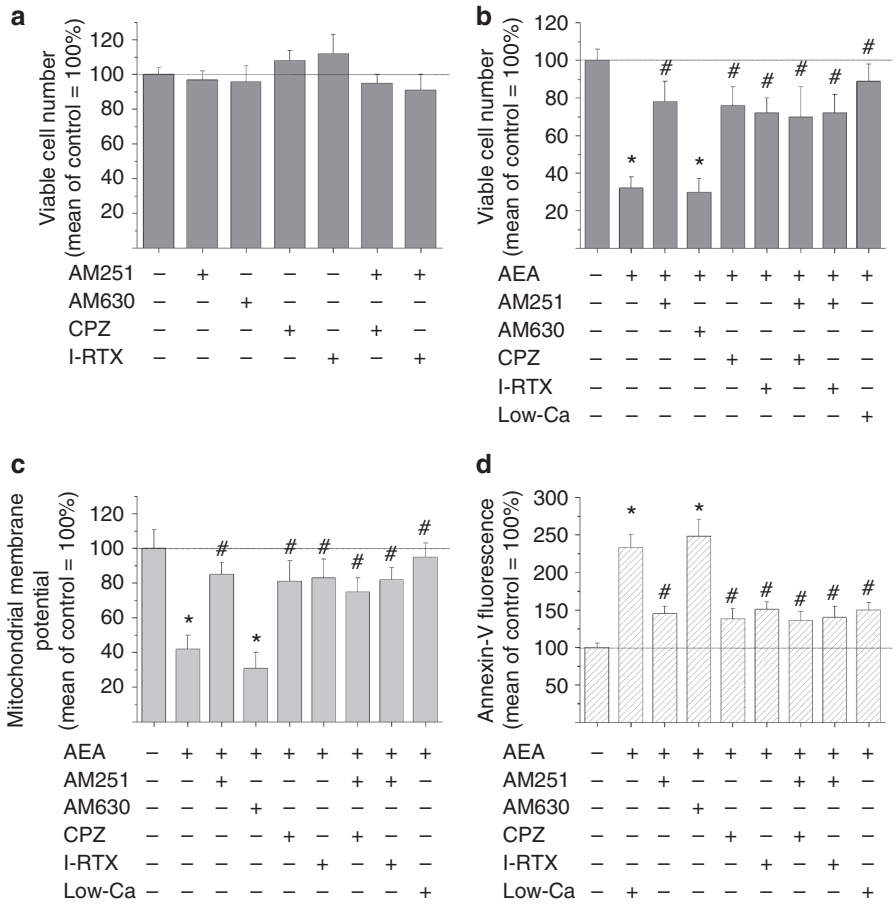

Figure 4. Cellular effects of *N*-arachidonoylethanolamine (AEA) are inhibited by antagonists of CB_1 and transient receptor potential vanilloid-1 (TRPV1), and by the suppression of extracellular $[Ca^{2+}]$. HaCaT keratinocytes (KCs) were treated for 24 hours by vehicle (control), 10 μM AEA, various antagonists: CB_1, 1 μM AM251; CB_2, 1 μM AM630; TRPV1, 5 μM capsazepine (CPZ); and 50 nM iodoresiniferatoxin (I-RTX). In addition, the effect of suppressing the $[Ca^{2+}]$ of the culturing medium from 2 to 0.02 mM (low-Ca) was also assessed. (**a**,**b**) Determination of viable cell number by MTT (3-(4,5-dimethylthiazol-2-yl)-2, 5-diphenyltetrazolium bromide) assay. Quantitative measurement of apoptosis by (**c**) $DiIC_1(5)$ assay and (**d**) Annexin-V assay. In all cases, data (mean ± SEM) are expressed as a percentage of the mean value (defined as 100%) of the vehicle-treated control group. For statistical analysis, * marks significant ($P<0.05$) differences compared with the vehicle-treated control group, whereas # marks significant ($P<0.05$) differences compared with the AEA-treated group; $n=4$ in each group. Three to four additional experiments yielded similar results.

MATERIALS AND METHODS

Materials

AEA, AM-251, CAPS, capsazepine, and iodoresiniferatoxin were purchased from Sigma-Aldrich (St Louis, MO); AM630 was obtained from Tocris (Ellisville, MO).

Cell culturing

Human skin samples were obtained after obtaining written informed consent from healthy individuals undergoing dermatosurgery, adhering to Helsinki guidelines, and after obtaining Institutional Research Ethics Committee's permission. NHEKs were isolated after overnight dermo-epidermal separation in 2.4 U ml^{-1} dispase (Roche Diagnostics, Berlin, Germany) by short trypsin (0.05%, Sigma-Aldrich) digestion. Cells were cultured in EpiLife serum-free medium (Invitrogen, Paisley, UK), supplemented with 1 μM insulin, 1 μM cortisol (both from Sigma-Aldrich), 100 μg ml^{-1} streptomycin, 100 U ml^{-1} penicillin, 50 ng ml^{-1} amphotericin B (all from Biogal, Debrecen, Hungary), 0.4% bovine pituitary extract (Invitrogen), and 0.06 mM $CaCl_2$ (Sigma-Aldrich).

Human immortalized HaCaT KCs were cultured in DMEM (Sigma-Aldrich) supplemented with 10% fetal calf serum, 2 mM L-glutamine, and antibiotics (all from Invitrogen; Bodó *et al.*, 2005; Gönczi *et al.*, 2008; Kiss *et al.*, 2008; Szegedi *et al.*, 2009).

Experiments on full-thickness human skin organ cultures

Human skin fragments of standardized size and volume were generated and cultured in serum-free Williams' E medium (Biochrom, Cambridge, UK) supplemented with 2 mM L-glutamine, 10 ng ml^{-1} hydrocortisone (Sigma-Aldrich), 10 μg ml^{-1} insulin, and penicillin/streptomycin solution (PAA Laboratories, Pasching, Austria; Lu *et al.*, 2007; Tiede *et al.*, 2009).

To simultaneously assess proliferation and apoptosis in human skin organ cultures, a Ki67/TUNEL double-staining method was employed (Foitzik *et al.*, 2000; Lindner *et al.*, 2000; Bodó *et al.*, 2005). Briefly, after AEA treatment, cryostat sections were first labeled with a digoxigenin–dUTP (ApopTag Fluorescein *In Situ* Apoptosis Detection Kit, Millipore, Billerica, MA) in the presence of terminal deoxynucleotidyl transferase and then with a mouse

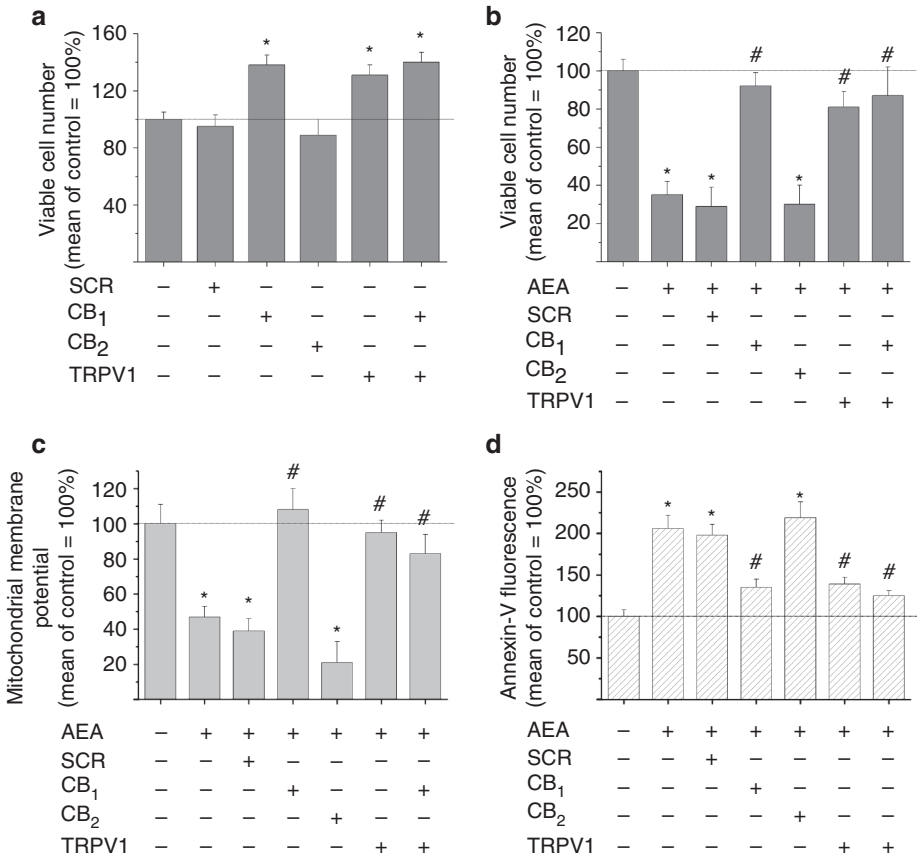

Figure 5. Cellular effects of *N*-arachidonoylethanolamine (AEA) are inhibited by RNA interference (RNAi)-mediated silencing of CB_1 and transient receptor potential vanilloid-1 (TRPV1), but not of CB_2. RNAi probes against CB_1, CB_2, and TRPV1, as well as scrambled RNAi probes (SCR), were introduced to HaCaT keratinocytes. Two days after transfection, cells were treated by 10 μM AEA for 24 hours. (**a**, **b**) Determination of viable cell number by colorimetric MTT (3-(4,5-dimethylthiazol-2-yl)-2,5-diphenyltetrazolium bromide) assay. Quantitative measurement of apoptosis by (**c**) $DiIC_1(5)$ assay and (**d**) Annexin-V assay. In all cases, data (mean ± SEM) are expressed as a percentage of the mean value (defined as 100%) of the vehicle-treated control group. For statistical analysis, * marks significant ($P<0.05$) differences compared with the SCR group, whereas # marks significant ($P<0.05$) differences compared with the AEA + SCR group; $n=4$ in each group. Three additional experiments yielded similar results.

anti-Ki67 antiserum (1:20, DAKO, Hamburg, Germany). TUNEL + cells were visualized by an anti-digoxigenin FITC-conjugated antibody (ApopTag kit), whereas Ki67 + cells were labeled with a rhodamine-conjugated goat anti-mouse secondary antibody (1:200, Jackson ImmunoResearch, West Grove, PA). Sections were then counterstained with DAPI (4′,6-diamidino-2-phenylindole; Vector Laboratories, Burlingame, CA). Negative controls were performed by omitting terminal deoxynucleotidyl transferase and the Ki67 antibodies. The analysis for cell counting on 10 sections per group was performed using a fluorescence microscope BZ-8100 (Biozero, Keyence, Osaka, Japan). The distance between two analyzed sections was more than 50 μm.

Immunocytochemistry

NHEK and HaCaT KCs were incubated with rabbit primary antibodies against CB_1, CB_2 (1:200 dilution, Cayman, Ann Arbor, MI), and TRPV1 (1:100, Sigma-Aldrich). For fluorescence staining, slides were then incubated with FITC-conjugated secondary antibodies (dilution 1:200, Vector Laboratories) and the nuclei were visualized using DAPI. As negative controls, the appropriate antibody was either omitted from the procedure or was pre-incubated with synthetic blocking peptides used in two times excess concentrations for 1 hour. (Figure 1a, insets; Bodó *et al.*, 2005; Dobrosi *et al.*, 2008; Tóth *et al.*, 2009).

Western blotting

KCs were harvested and lysed in ice-cold lysis buffer (20 mM Tris-HCl (pH 7.5), 5 mM EGTA, protease inhibitor cocktail 1:100, all from Sigma-Aldrich). After determining the protein content, 100 μg protein from each sample was subjected to SDS-PAGE, transferred to BioBond nitrocellulose membranes (Whatman, Maidstone, UK), and then probed with the above-mentioned antibodies against CB_1, CB_2 (both in the ratio 1:200) and TRPV1 (1:100). A horseradish peroxidase-conjugated goat anti-rabbit IgG antibody (1:1,000, Bio-Rad, Hercules, CA) was used as a secondary antibody, and the immunoreactive bands were visualized by a SuperSignal West Pico Chemiluminescent Substrate-Enhanced Chemiluminescence kit (Pierce, Rockford, IL) using LAS-3000 Intelligent Dark Box (Fuji, Tokyo, Japan). To assess equal loading, membranes were re-probed with an anti-cytochrome *c* antibody (1:50, Santa Cruz Biotechnology, Santa Cruz, CA) and visualized as described above.

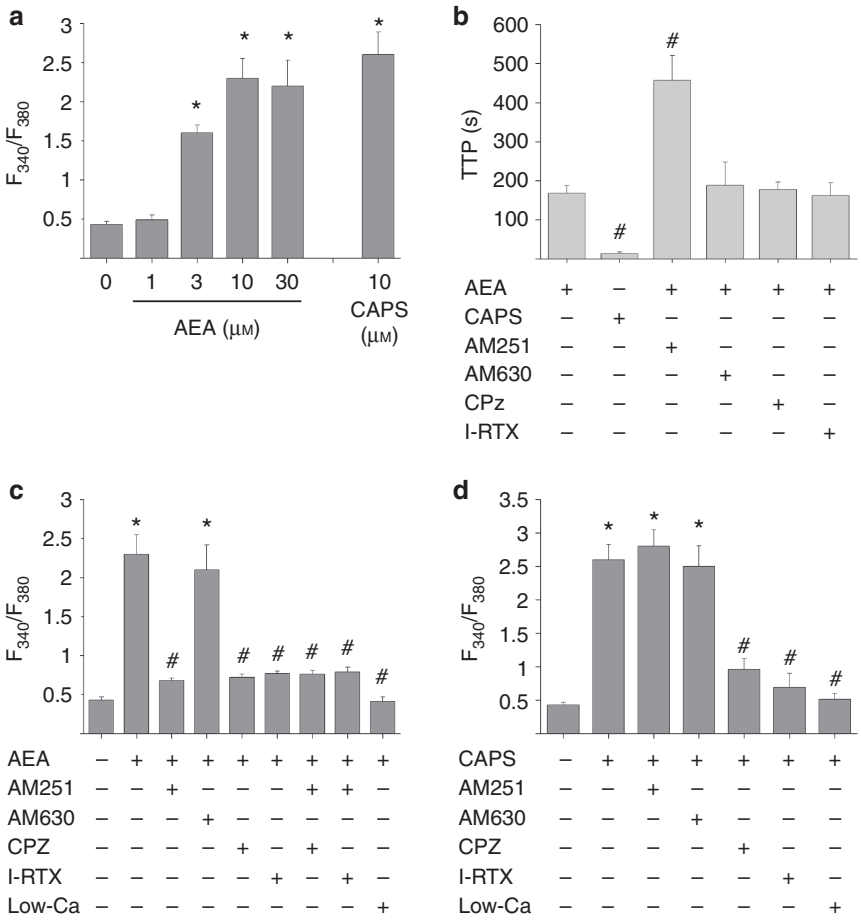

Figure 6. *N*-arachidonoylethanolamine (AEA) induces elevations of intracellular Ca^{2+} concentration ($[Ca^{2+}]_i$) by antagonists of CB_1 and transient receptor potential vanilloid-1 (TRPV1), and by the suppression of extracellular $[Ca^{2+}]$. Ca^{2+} imaging on fura-2-loaded HaCaT keratinocytes. Fluorescence ratio (F_{340}/F_{380}) values of excitations at 340 and 380 nm wavelengths were recorded. (**a**) Effects of increasing doses on AEA and 10 μM capsaicin (CAPS). (**b**, **c**) Effects of various antagonists (CB_1: 1 μM AM251; CB_2: 1 μM AM630; TRPV1: 5 μM CPZ; and 50 nM I-RTX) as well as of suppressing the $[Ca^{2+}]$ of the medium from 2 to 0.02 mM (low-Ca) on the time-to-peak (TTP) values (**b**) and amplitudes (**c**) of Ca^{2+} transients evoked by 10 μM AEA. (**d**) Effects of antagonists and of suppressing extracellular $[Ca^{2+}]$ on the amplitudes of Ca^{2+} transients evoked by 10 μM CAPS. In all cases, mean ± SEM of multiple determinations ($n>10$ cells) are presented. For statistical analysis, * marks significant ($P<0.05$) differences compared with the vehicle-treated group, whereas # marks significant ($P<0.05$) differences compared with the AEA-treated (**b**,**c**) or CAPS-treated (**d**) groups.

RT-PCR

Total RNA was isolated using TRIzol (Invitrogen), and the isolated total RNA was reverse-transcribed into cDNA and then amplified on a GeneAmp PCR System 2400 DNA Thermal Cycler (Applied Biosystems, Foster City, CA). Primers were synthesized by Invitrogen (CB_1, forward: 5′-CAAGCCCGCATGGACATTAGGTTA-3′, reverse: 5′-TCCGAGTCCCCCATGCTGTTATC-3′, 291 bp, accession number: NM_016083.4, non-intronspanning; CB_2, forward: 5′-TCCCACTGA TCCCCAATGACTACC-3′, reverse: 5′-AGGATCTCGGGGCTTCT TCTTTTG-3′, 459 bp, accession number: NM_001841.2, non-intronspanning; TRPV1 forward: 5′-CTCCTACAACAGCCTGTAC-3′, reverse: 5′-AAGGCCCAGTGTTGACAGTG-3′, 680 bp, accession number: NM_080704.3, intronspanning; glyceraldehyde-3-phosphate dehydrogenase, forward: 5′-ATGGTGAAGGTCGGTGTGAAC-3′, reverse: 5′-GCTGACAATCTTGAGGGAGT-3′, 340 bp, accession number: NM_002046.3, non-intronspanning). PCR products were visualized on 1.5% agarose gel with ethidium bromide (0.5 mg ml^{-1}, Sigma-Aldrich) under UV light.

Determination of viable cell numbers and proliferation

Cells were plated in 96-well multi-titer plates (20,000 cells per well density, which corresponded to approximately 70–80% confluence) in quadruplicates, and the number of viable cells (hence, the rate of proliferation) was determined by measuring the conversion of the tetrazolium salt MTT (3-(4,5-dimethylthiazol-2-yl)-2,5-diphenyl-tetrazolium bromide; Sigma-Aldrich) to formazan by mitochondrial dehydrogenases (Tóth *et al.*, 2009). In all cases, experiments were repeated at least three times.

Determination of apoptosis

A decrease in the mitochondrial membrane potential is one of the earliest markers of apoptosis (Green and Reed, 1998; Susin *et al.*, 1998). Mitochondrial membrane potential of cells was determined using a MitoProbe $DiIC_1(5)$ Assay Kit (Invitrogen). Cells (20,000 cells per well) were cultured in 96-well plates and treated in quadruplicates. After treatment, cells were incubated for 30 minutes with $DiIC_1(5)$ dye. Fluorescence was measured at 630 nm excitation and

670 nm emission wavelengths using a fluorescence image plate reader (FLIPR; Molecular Devices, San Francisco, CA).

In addition, apoptosis was also assessed by measuring phosphatidylserine translocation with FITC-conjugated Annexin-V (1:100, Sigma-Aldrich). Fluorescence was measured at 490 nm excitation and 520 nm emission wavelengths using FLIPR. As a complementary approach, immunocytochemistry was also performed using the same labeling method (data not shown).

Finally, apoptosis was also determined by fluorimetric measurement of activation of pro-apoptotic caspases using a fluorescent inhibitor of caspases (FLICA methodology, Poly Caspases Detection Kit, Invitrogen). The fluorescent FLICA reagent specifically and covalently interacts with the active centers of activated caspases via a caspase-specific recognition sequence. KCs were incubated with FLICA reagent and fluorescence was measured at 490 nm excitation and 530 nm emission wavelengths using FLIPR (Dobrosi *et al.*, 2008; Tóth *et al.*, 2009). In all apoptosis assays, experiments were repeated at least three times.

Determination of cytotoxicity (necrosis)

Cells (20,000 cells per well) were cultured in 96-well plates and treated in quadruplicates with endocannabinoids and antagonists for 24 hours. Necrotic cell death was determined by measuring G6PD release by an enzymatic process that leads to the reduction of resazurin into red-fluorescent resorufin (G6PD Release Assay Kit, Invitrogen). Fluorescence emission of resorufin was monitored by the FLIPR device at 545 excitation and 590 emission wavelengths.

As the activity of the G6PD released from necrotic cells decreases over 24 hours, the cytotoxic effects of long-term treatment protocols were determined by Sytox Green staining (Invitrogen). The dye is able to penetrate (and then bind to the nucleic acids) only into necrotic cells with ruptured plasma membranes. Fluorescence of intranuclear SYTOX Green was measured at 490 nm excitation and 520 nm emission wavelengths using a FLIPR (Dobrosi *et al.*, 2008; Tóth *et al.*, 2009). In both cytotoxicity assays, experiments were repeated at least three times.

RNA interference

RNAi was performed according to our optimized protocols (Dobrosi *et al.*, 2008; Tóth *et al.*, 2009). In brief, KCs at 50–70% confluence were transfected with specific stealth RNAi oligonucleotides (40 nM) against CB_1 (ID no. HSS102082), CB_2 (ID no. HSS102087), and TRPV1 (ID no. HSS111305) using Lipofectamine 2000 (all from Invitrogen). For controls, RNAi-negative control duplexes (scrambled RNAi) were employed. The efficacy of RNAi-driven ''knockdown'' was daily evaluated by quantitative PCR and western blotting for 4 days. At days 2 and 3, all specific RNAi oligonucleotides resulted in >70% silencing of the given molecule (see Supplementary Figure 2 online and Supplementary Data online).

Calcium measurement

Changes in $[Ca^{2+}]_i$ on TRPV1 activation were detected as described before (Bodó *et al.*, 2005; Tóth *et al.*, 2009). KCs, cultured on glass coverslips, were loaded with a calcium-sensitive probe fura-2 AM (5 μM, Invitrogen) and were then placed on the stage of an inverted fluorescence microscope (Diaphot, Nikon, Tokyo, Japan). Excitation was alternated between 340 and 380 nm using a dual-wavelength monochromator (Deltascan, Photon Technology International, New Brunswick, NJ). The emission was monitored at 510 nm with a photomultiplier at an acquisition rate of 10 Hz per ratio, and the fluorescence ratio (F_{340}/F_{380}) values were determined. Experiments were carried out on >10 cells in each experimental group.

Statistical analysis

Data were analyzed using one-way ANOVA with Bonferroni's and Dunnett's *post hoc* probes, and $P<0.05$ values were regarded as significant differences.

CONFLICT OF INTEREST

The authors state no conflict of interest.

ACKNOWLEDGMENTS

This work was supported, in part, by Hungarian (OTKA NK78398, OTKA NNF78456, TÁMOP-4. 2.2-08/1/2008-0019, TÁMOP 4.2.1./B-09/1/KONV-2010-0007) and EU (FP7-REGPOT-2008-1/22992) research grants for TB and by the Deutsche Forschungsgemeinschaft to RP. TB and GC are recipients of the János Bolyai scholarship of the Hungarian Academy of Sciences.

SUPPLEMENTARY MATERIAL

Supplementary material is linked to the online version of the paper at http://www.nature.com/jid

REFERENCES

Berdyshev EV, Schmid PC, Dong Z *et al.* (2000) Stress-induced generation of N-acylethanolamines in mouse epidermal JB6 P+ cells. *Biochem J* 346:369–74

Bíró T, Tóth IB, Haskó G *et al.* (2009) The endocannabinoid system of the skin in health and disease: novel perspectives and therapeutic opportunities. *Trends Pharmacol Sci* 30:411–20

Blazquez C, Carracedo A, Barrado L *et al.* (2006) Cannabinoid receptors as novel targets for the treatment of melanoma. *FASEB J* 20:2633–5

Bodó E, Bíró T, Telek A *et al.* (2005) A ''hot'' new twist to hair biology—involvement of vanilloid receptor-1 (VR1/TRPV1) signaling in human hair growth control. *Am J Pathol* 166:985–98

Calignano A, La Rana G, Giuffrida A *et al.* (1998) Control of pain initiation by endogenous cannabinoids. *Nature* 394:277–81

Casanova ML, Blazquez C, Martinez-Palacio J *et al.* (2003) Inhibition of skin tumor growth and angiogenesis *in vivo* by activation of cannabinoid receptors. *J Clin Invest* 111:43–50

Di Marzo V (2008) Targeting the endocannabinoid system: to enhance or reduce? *Nat Rev Drug Discov* 7:438–55

Di Marzo V, Bisogno T, De Petrocellis L (2001) Anandamide: some like it hot. *Trends Pharmacol Sci* 22:346–9

Di Marzo V, Bisogno T, Melck D *et al.* (1998) Interactions between synthetic vanilloids and the endogenous cannabinoid system. *FEBS Lett* 436: 449–54

Dobrosi N, Tóth IB, Nagy G *et al.* (2008) Endocannabinoids enhance lipid synthesis and apoptosis of human sebocytes via cannabinoid receptor-2-mediated signaling. *FASEB J* 22:3685–95

Fioravanti B, De Felice M, Stucky CL *et al.* (2008) Constitutive activity at the cannabinoid CB1 receptor is required for behavioral response to noxious chemical stimulation of TRPV1: antinociceptive actions of CB1 inverse agonists. *J Neurosci* 28:11593–602

Foitzik K, Lindner G, Müller-Röver S *et al.* (2000) Control of murine hair follicle regression (catagen) by TGF-beta1 *in vivo*. *FASEB J* 14: 752–60

Green DR, Reed JC (1998) Mitochondria and apoptosis. *Science* 281: 1309–12

Gönczi M, Telek A, Czifra G *et al.* (2008) Altered calcium handling following the recombinant overexpression of protein kinase C isoforms in HaCaT cells. *Exp Dermatol* 17:584–91

Hermann H, De Petrocellis L, Bisogno T *et al.* (2003) Dual effect of cannabinoid CB1 receptor stimulation on a vanilloid VR1 receptor-mediated response. *Cell Mol Life Sci* 60:607–16

Howlett AC (2005) Cannabinoid receptor signaling. *Handb Exp Pharmacol* 168:53–79

Howlett AC, Barth F, Bonner TI *et al.* (2002) International Union of Pharmacology. XXVII. Classification of cannabinoid receptors. *Pharmacol Rev* 54:161–202

Ibrahim MM, Porreca F, Lai J *et al.* (2005) CB2 cannabinoid receptor activation produces antinociception by stimulating peripheral release of endogenous opioids. *Proc Natl Acad Sci USA* 102:3093–8

Karsak M, Gaffal E, Date R *et al.* (2007) Attenuation of allergic contact dermatitis through the endocannabinoid system. *Science* 316:1494–7

Kiss B, Bíró T, Czifra G *et al.* (2008) Investigation of micronized titanium-dioxide penetration in human skin xenografts and its effect on cellular functions of human skin-derived cells. *Exp Dermatol* 17:659–67

Kupczyk P, Reich A, Szepietowski JC (2009) Cannabinoid system in the skin – a possible target for future therapies in dermatology. *Exp Dermatol* 18:669–79

Lazar J, Braun DC, Toth A *et al.* (2006) Kinetics of penetration influence the apparent potency of vanilloids on TRPV1. *Mol Pharmacol* 69:1166–73

Lindner G, Menrad A, Gharadi E *et al.* (2000) Involvement of hepatocyte growth factor/scatter factor and met receptor signaling in hair follicle morphogenesis and cycling. *FASEB J* 14:319–32

Lu Z, Hasse S, Bodó E *et al.* (2007) Towards the development of a simplified long-term organ culture method for human scalp skin and its appendages under serum-free conditions. *Exp Dermatol* 16:37–44

Maccarrone M, Di Rienzo M, Battista N *et al.* (2003) The endocannabinoid system in human keratinocytes. Evidence that anandamide inhibits epidermal differentiation through CB1 receptor-dependent inhibition of protein kinase C, activation protein-1, and transglutaminase. *J Biol Chem* 278:33896–903

Mackie K (2006) Cannabinoid receptors as therapeutic targets. *Annu Rev Pharmacol Toxicol* 46:101–22

Mechoulam R, Fride E, Di Marzo V (1998) Endocannabinoids. *Eur J Pharmacol* 359:1–18

Oka S, Wakui J, Ikeda S *et al.* (2006) Involvement of the cannabinoid CB2 receptor and its endogenous ligand 2-arachidonoylglycerol in oxazolone-induced contact dermatitis in mice. *J Immunol* 177:8796–805

Pacher P, Batkai S, Kunos G (2006) The endocannabinoid system as an emerging target of pharmacotherapy. *Pharmacol Rev* 58:389–462

Paradisi A, Pasquariello N, Barcaroli D *et al.* (2008) Anandamide regulates keratinocyte differentiation by inducing DNA methylation in a CB1 receptor dependent manner. *J Biol Chem* 283:6005–12

Pertwee RG (2005) Pharmacological actions of cannabinoids. *Handb Exp Pharmacol* 168:1–51

Petrosino S, Cristino L, Karsak M *et al.* (2010) Protective role of palmitoylethanolamide in contact allergic dermatitis. *Allergy* 65:698–711

Slominski A, Wortsman J (2000) Neuroendocrinology of the skin. *Endocr Rev* 21:457–87

Slominski A, Wortsman J, Paus R *et al.* (2008) Skin as an endocrine organ: implications for its function. *Drug Discov Today Dis Mech* 5: 137–44

Southall MD, Li T, Gharibova LS *et al.* (2003) Activation of epidermal vanilloid receptor-1 induces release of proinflammatory mediators in human keratinocytes. *J Pharmacol Exp Ther* 304:217–22

Stander S, Schmelz M, Metze D *et al.* (2005) Distribution of cannabinoid receptor 1 (CB1) and 2 (CB2) on sensory nerve fibers and adnexal structures in human skin. *J Dermatol Sci* 38:177–88

Susin SA, Zamzami N, Kroemer G (1998) Mitochondria as regulators of apoptosis: doubt no more. *Biochem Biophys Acta* 1366:151–65

Szegedi A, Páyer E, Czifra G *et al.* (2009) Protein kinase C isoenzymes differentially regulate the differentiation-dependent expression of adhesion molecules in human epidermal HaCaT keratinocytes. *Exp Dermatol* 18:122–9

Telek A, Bíró T, Bodó E *et al.* (2007) Inhibition of human hair follicle growth by endo- and exocannabinoids. *FASEB J* 21:3534–41

Tiede S, Kloepper JE, Ernst N *et al.* (2009) Nestin in human skin: exclusive expression in intramesenchymal skin compartments and regulation by leptin. *J Invest Dermatol* 129:2711–20

Tóth IB, Géczy T, Griger Z *et al.* (2009) Transient receptor potential vanilloid-1 signaling as a regulator of human sebocyte biology. *J Invest Dermatol* 129:329–39

Ursu D, Knopp K, Beattie RE *et al.* (2010) Pungency of TRPV1 agonists is directly correlated with kinetics of receptor activation and lipophilicity. *Eur J Pharmacol* 641:114–22

Wilkinson JD, Williamson EM (2007) Cannabinoids inhibit human keratinocyte proliferation through a non-CB1/CB2 mechanism and have a potential therapeutic value in the treatment of psoriasis. *J Dermatol Sci* 45:87–92

Zygmunt PM, Petersson J, Andersson DA *et al.* (1999) Vanilloid receptors on sensory nerves mediate the vasodilator action of anandamide. *Nature* 400:452–7